Spatially variant changes in lens power during ocular accommodation in a rhesus monkey eye

Abhiram S. Vilupuru

College of Optometry, University of Houston, Houston, TX, USA

 \bowtie

Austin Roorda

College of Optometry, University of Houston, Houston, TX, USA



College of Optometry, University of Houston, Houston, TX, USA



Adrian Glasser

This study investigated the changes in ocular aberrations that occur over the entire lens equatorial diameter during accommodation in iridectomized rhesus monkey eyes to understand the nature of accommodative lenticular deformation. Accommodation was centrally stimulated to a range of different response amplitudes (0 D to ~ 11 D), and ocular aberrations were measured with a Shack-Hartmann wavefront sensor in both eyes of one previously iridectomized 10-year-old rhesus monkey. At the highest amplitude in the two eyes, aberrations were analyzed over entrance pupil diameters ranging from 3 to 8 mm in steps of 1 mm. Root mean square error of the total measured aberrations, excluding defocus, increased systematically with increasing accommodation from about 1 to 3.5 microns. Spherical aberration became systematically more negative, and vertical coma increased significantly in magnitude with accommodation. There was a strong accommodative change in power near the center of the lens and little change in power at the periphery. At the highest accommodative state, decreasing the analyzed entrance pupil diameter from 8 to 3 mm considerably reduced the wavefront error. The greater increase in optical power near the central region of the lens, combined with an accommodative pupillary miosis, would serve to maximize accommodative refractive change while maintaining acceptable image quality.

Keywords: accommodation, crystalline lens, wave aberration, spherical aberration

Introduction

Accommodation is the dynamic change in optical power of the eye that allows objects at different distances in the visual field to be focused on the retinal image plane. In primates, the change in optical power is brought about by a change in the shape of the crystalline lens (Glasser & Campbell, 1998; Glasser & Kaufman, 1999; Helmholtz, 1924; Young, 1801). The mechanism of accommodation in humans as originally postulated by Helmholtz (Helmholtz, 1924) is widely accepted. Helmholtz proposed that during accommodation the ciliary muscle contracts, releasing tension on the zonular fibers at the lens equator, allowing the lens equatorial diameter to decrease, the lens thickness to increase, and the lens anterior surface to become more steeply curved. Helmholtz described the lens substance as elastic and ascribed no role in accommodation to the lens capsule, the thin elastic membrane surrounding the lens. Gullstrand (1924) elaborated on the Helmholtz accommodative mechanism and recognized the importance of the role of the capsule in accommodating the lens. Tscherning (1920), from studying images reflected from the anterior lens surface and from his own experience of how the image structure of his eye changed with accommodation, suggested that the accommodative mechanism in primates is

fundamentally different from that described by Helmholtz. Tscherning believed that the lens center became more steeply curved, but the lens periphery flattened with accommodation and proposed that ciliary muscle contraction increased zonular tension to increase lens equatorial diameter to cause this paradoxical accommodative change in lens shape. This theory of accommodation has received renewed attention (Schachar, Black, Kash, Cudmore, & Schanzlin, 1995; Schachar, Tello, Cudmore, Liebmann, Black, & Ritch, 1996), but subsequent experimental evidence demonstrates that the lens equatorial diameter decreases with accommodation to provide further evidence in favor of the Helmholtz theory (Glasser & Kaufman, 1999). MRI studies and infrared retroillumination of the eye of a subject with ocular albinism also show a decrease in lens equatorial diameter with accommodation (Strenk & Semmlow, 1995; Wilson, 1997).

Fincham (1937b) recognized the role of the capsule in changing the shape of the lens during accommodation. Fincham studied the lens capsules of several species and described a variation in capsular thickness, with the thinnest parts near the center of the lens anterior and posterior surfaces and a mid-peripheral thickening in the capsules of accommodating species that was not present in the capsules of nonaccommodating species. Fincham stated that the

elastic capsule "presses upon the soft lens-substance and moulds it into the accommodated form by compressing it at the equator and in those regions where the capsule is thickest, allowing it to bulge in the thinner parts (Fincham, 1937b)."

Previous studies in humans have shown that ocular aberrations change during accommodation because the lens changes shape (Atchison, Collins, Wildsoet, Christensen, & Waterworth, 1995; He, Burns, & Marcos, 2000; Ninomiya et al., 2002; Pallikaris, Panagopoulou, Siganos, & Molebny, 2001). Spherical aberration, in particular, has been shown to become less positive or more negative during accommodation (He et al., 2000; Ivanoff, 1947; Jenkins, 1963; Koomen, Tousey, & Scolnik, 1949; Lopez-Gil, Iglesias, & Artal, 1998; Ninomiya et al., 2002; Pallikaris et al., 2001; van den Brink, 1962). In vitro mechanical stretching experiments designed to simulate accommodative changes in the lens in enucleated human and rhesus monkey eyes show that negative spherical aberration increases when stretching tension is released and the lenses are allowed to become accommodated (human, Glasser & Campbell, 1998; rhesus monkey, Roorda & Glasser, 1999; Roorda & Glasser, 2004).

The iris normally obscures the lens periphery and reduces the entrance pupil diameter through which ocular aberrations can be measured. In addition, because the pupil normally constricts with accommodation, the entrance pupil diameter through which ocular aberrations can be measured decreases as the eye accommodates. Understanding the accommodative changes in optical aberrations over the entire lens diameter may help to understand the exact nature of lenticular changes during accommodation and may reconcile some aspects of the differing accommodative theories. Although the pupil diameter can be increased with phenylephrine without blocking accommodation, this still does not reveal the full diameter of the lens nor does it completely block accommodative pupillary constriction. Thus the lens periphery remains obscured. Surgical iridectomy in rhesus monkey eyes completely removes the iris (Kaufman & Lütjen-Drecoll, 1975) and has allowed visualization of the accommodative movements of the ciliary processes and the lens equator. Surgical iridectomy offers the opportunity to measure the ocular aberrations over the full diameter of the lens unencumbered by the presence of the iris.

Rhesus monkeys have high accommodative amplitudes and an accommodative apparatus and mechanism similar to that of human eyes (Bito, Kaufman, DeRousseau, & Koretz, 1987). Prior studies have used mid-brain electrical stimulation of the Edinger-Westphal (EW) nucleus in anesthetized monkeys to study accommodative changes in surgically iridectomized eyes (Crawford, Kaufman, & Bito, 1990; Croft et al., 1998; Glasser & Kaufman, 1999). EW stimulation produces an accommodative contraction of the ciliary muscle through stimulation of the preganglionic, parasympathetic neurons that innervate the eye and allows rigorous control over the amplitude and duration of the

accommodative response through control of the frequency, amplitude, and duration of the stimulus current. Surgical iridectomy does not alter the accommodative mechanism or the EW stimulated accommodative response amplitude (Crawford et al., 1990; Glasser & Kaufman, 1999). In the present study, changes in optical aberrations have been measured over the entire lens diameter during electrically stimulated accommodation in the two iridectomized eyes of a rhesus monkey.

Methods

All experiments conducted conformed to the ARVO Statement for the Use of Animals in Ophthalmic and Vision Research and were performed in accordance with institutionally approved animal protocols. Experiments were conducted on one adolescent rhesus monkey aged 10 years. The irides of the two eyes had been previously surgically removed (Kaufman & Lütjen-Drecoll, 1975) and a stimulating electrode had previously been surgically implanted in the EW nucleus of the brain (Crawford, Terasawa, & Kaufman, 1989; Vilupuru & Glasser, 2002).

The monkey was anesthetized (intramuscular 10 mg/kg ketamine and 0.5 mg/kg acepromazine followed by intravenous 15 mg/kg sodium pentobarbital with hourly supplements of 10 mg/kg as required to maintain surgical depth anesthesia) and placed prone in a head holder, with the head upright and facing forward. The eyelids were held open with lid speculums. Light tension was placed on sutures passed beneath the medial and lateral extraocular muscles to minimize accommodative convergent eye movements. Plano, rigid, contact lenses were placed on the corneas to prevent dehydration and loss of optical clarity during the experiment.

An accommodation stimulus response function was first generated for each eve by delivering gradually increasing stimulus currents to the EW nucleus and recording the accommodative responses of each eye with a Hartinger coincidence refractometer (Fincham, 1937a; Vilupuru & Glasser, 2002). The Hartinger, a Scheiner principle optometer, measures the refraction of the eye through a fixed 1-2 mm entrance pupil diameter, and so even in an iridectomized eye measures the paraxial change in power rather than the total change in power over the full iridectomized entrance pupil diameter. Stimulus current amplitudes ranging from zero µA (to produce no accommodation) up to 640 uA (to produce maximum accommodation) were used. Infrared photorefraction was used to record dynamic accommodative responses and to observe and demonstrate an accommodative decrease in lens equatorial diameter (Glasser & Kaufman, 1999; Vilupuru & Glasser, 2002). Ocular aberrations were measured in multiple different accommodative states (right eye, 10; left eye, 8) ranging from zero accommodation (unaccommodated) to maximally accommodated. The aberrations were measured with a Shack-Hartmann wavefront sensor (SHWS) designed and

built by author AR (Liang, Grimm, Goelz, & Bille, 1994; Liang & Williams, 1997), placed in front of the eye. Alignment of the HSWS with the optical axis of the eye was achieved by using an integrated video camera to monitor the eye, equatorial diameter of the lens, and the corneal reflex from a coaxial light source. Careful adjustment of the eye via the extraocular muscle sutures and the instrument was made to ensure that the corneal reflex remained centered with the visible aperture of the equatorial edge of the lens.

The SHWS projects a narrow, low-intensity laser beam onto the retina. The light scattered from the retina serves as a secondary source and passes back through the optics of the eye (crystalline lens and cornea). The emergent wavefront at the entrance pupil of the eye is imaged with a lenslet array (400 micrometer spacing, 24-mm focal length), which produces an array of focused spots onto a CCD chip. The x, y deviation of each spot from its ideal location (i.e., for an aberration-free wavefront) indicates the local slope of the wavefront at that corresponding lenslet. Stimulus pulse trains, 4 s in duration, were delivered to the EW nucleus to induce accommodative responses. When the eye reached a stable accommodated level (about 3 s after stimulus onset), SHWS images were captured. For each different stimulus amplitude (and therefore accommodated state) five images were captured, one each from five successive 4-s long stimulations.

Captured images were analyzed to determine the ocular aberrations over the entire lens diameter in the iridectomized eyes for all accommodated states. Wavefront slope data from each spot pattern were fitted with a series of Zernike polynomials (Cubalchini, 1979; Liang et al., 1994) (up to 10th order) over an entrance pupil diameter of 8 mm using a custom written software program. The specific Zernike terms and their ordering were from the accepted standard for use in vision science (Thibos, Applegate, Schwiegerling, Webb, & VSIA Standards Taskforce Members, 2001). Each Zernike term corresponds to a particular aberration and the coefficient of that term indicates the contribution of that aberration to the overall wavefront error.

Coefficients of each of the Zernike terms obtained from all five images captured at the same stimulus amplitude were averaged. Wavefront maps were calculated at each increasing accommodative state to show the increase in aberrations with increasing accommodation. Point spread functions (PSFs) were estimated from the wavefront aberrations that were calculated from the measured aberrations. As a measure of the overall quality of the optics of the eye, the changes in higher order aberration terms, excluding defocus, were determined by calculating the root mean square (RMS) error of the wave aberration.

To calculate local optical power changes within the entire 8-mm entrance pupil diameter of the eye for each accommodative state, curvature maps were calculated as the second derivative of the wavefront maps at each amplitude,

from the unaccommodated state (0 µA) to the highest amplitude in each eye, using a custom written Matlab program. The curvature maps show local power changes over the entrance pupil (Thibos & Applegate, 2001). The curvature maps were converted to diopters by multiplication with an empirically derived constant of proportionality, which was 800 for our calculations. The converted curvature maps were then sampled in eight concentric annuli with radii from 0.5 mm out to 4 mm to encompass the full 8-mm entrance pupil diameter. The width of each annular region considered was 0.5 mm and the data within each annulus were averaged to provide one power value for that annulus. This analysis was done on each of the five SHWS images captured for each accommodated state to obtain a mean power of each annulus and a SD for the five images at each accommodated state.

To understand, in the iridectomized eye, how an accommodative pupil constriction would impact the ocular aberrations if the iris were present, five images at the highest accommodative state of each eye (right, 11 D; left, 9 D) were analyzed for entrance pupil diameters ranging from 8 to 3 mm in 1-mm steps.

Results

Infrared photorefraction video sequences of accommodation in the iridectomized eyes consistently show a systematic decrease in lens equatorial diameter during accommodation (Figure 1) (Glasser & Kaufman, 1999). The difference in appearance of the photorefraction fundus brightness changes between center and periphery during accommodation (Figure 1) suggests that there is an increase in optical power in the central region of the eye but little change at the periphery.

Similarly, the dynamic changes in the SHWS image spot pattern showed a clear compression near the center with accommodation (Figure 2a), also indicating a greater change in optical power near the center of the eye. The relatively rectilinear arrangement of SHWS spots in the unaccommodated state (Figure 2b) undergoes a greater compression toward the center to show increasing "pin cushion" distortion when the eye accommodates (Figure 2c).

As accommodation increases, there is an increase in the spherical equivalent refractive power of the eye which is evident from the increase in the fourth Zernike or defocus term (data not shown). Wavefront maps were calculated for each refractive state from unaccommodated to approximately 11 D of accommodation over an 8-mm entrance pupil diameter (Figure 3a). The wavefront maps (with spherical defocus removed) show an increase in aberrations over the 8-mm entrance pupil diameter. As accommodation increased, the size of the PSF increased, and the calculated Strehl ratio decreased systematically with increasing accommodation (Strehl ratios with increasing accommoda-

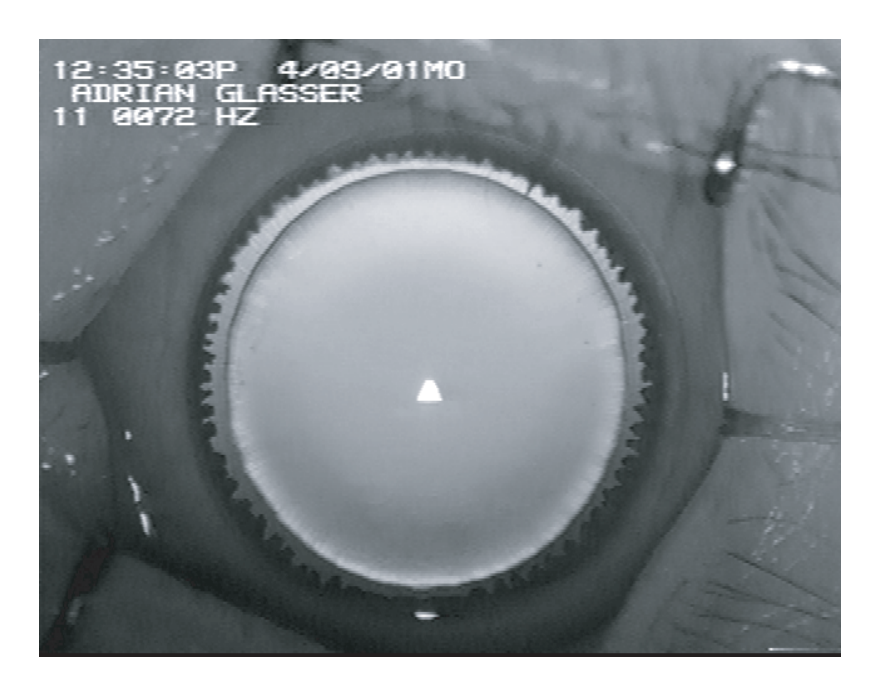


Figure 1. Video clip of infrared photorefraction recorded in the right eye during Edinger-Westphal nucleus stimulated accommodation to an amplitude of 10 D. The stimulus is presented for 4 s. The stimulus indicator "00" turns to "11" (at upper left) when the stimulus is delivered. The tips of the ciliary processes around the lens equator appear and the lens diameter decreases as the eye accommodates. The photorefractive image also shows that the refraction of the eye is changing to a greater degree near the center than at the periphery by virtue of the greater change in the photorefraction brightness gradient near the central region of the eye than at the periphery.

tion: 0.00652, 0.00641, 0.00213, 0.00224, and 0.00135) (Figure 3b). The radially symmetric wavefront aberration and larger PSF at the highest accommodative amplitude are primarily due to an increase in symmetric spherical aberration.

The RMS error of the wave aberration (excluding defocus) for both eyes increased systematically with accommodation (Figure 4), indicating an increase in ocular aberrations with accommodation. The increasing RMS wave aberration and the corresponding decrease in Strehl ratio indicate clearly that the quality of the monkey's optics over an 8-mm pupil degrades with accommodation.

There was a statistically significant increase in vertical coma $(Z_{3,-1})$ at the highest accommodative amplitude compared to the unaccommodated state in the two eyes (Figure 5a & 5b) (t test; OD: t = 19.77, p < .002; OS: t = 3.48, p < .05). Vertical coma changed systematically only in the right eye, whereas the left eye showed a significant change at the highest amplitude. Spherical aberration ($Z_{4,0}$: symmetric spherical aberration) became systematically more negative with accommodation in the two eyes. The magnitude of spherical aberration ($Z_{4,0}$) was statistically greater at the highest accommodative amplitude compared to the unaccommodated state (Figure 5c & 5d) (t test; OD: t = 18.6, p < .05; OS: t = 10.47, p < .05). The other fourth-order spherical aberration terms underwent small nonsystematic changes (Figure 5 c & d).

The local change in optical power over the entire lens diameter was calculated for each accommodated state by sampling the calculated curvature maps at each accommodative state over 1-mm annuli from the center to the periphery. The graphs of the right (Figure 6a) and left (Figure 6b) eyes show mean optical power for each refractive state at each concentric annular region from center to the periphery. With increasing stimulus amplitudes, there is an increase in optical power near the center of the eye, but with increasing eccentricity from the center, the accommodative change in power was progressively less in both eyes (Figure 6a & 6b). In some cases, the eye became more hyperopic in the periphery.

An analysis of the SHWS images from the maximally accommodated state showed that the wavefront aberrations decreased as the analyzed entrance pupil diameter was decreased as shown by a decrease in the RMS error and a reduction in the spread of the PSF (Figure 7 a & 7b). The extent of vertical coma ($Z_{3,-1}$) and spherical aberration ($Z_{4,0}$) decreased with the decrease in entrance pupil diameter (data not shown) in the same quadratic manner as does total RMS.

Discussion

In this study, ocular aberrations at different accommodative states were measured over a fixed entrance pupil diameter encompassing the full lens diameter in the two iridectomized eyes of a rhesus monkey to compare optical changes occurring over the full diameter of the lens. The monkey was initially anesthetized with ketamine + acepro-

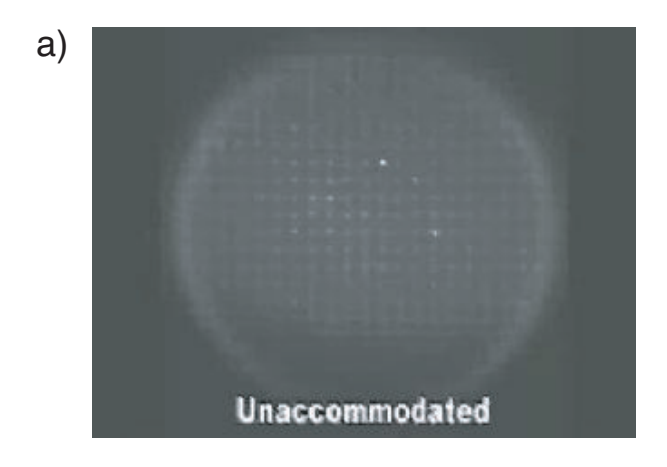
mazine. This was followed by induction of surgical depth anesthesia for the experiments. After the monkey was initially anesthetized with ketamine, aberrations were measured before and after induction of surgical depth anesthesia to ascertain if the increased depth of anesthesia would cause a change in aberrations. The ocular aberrations did not vary systematically before and after induction of surgical depth anesthesia. For the experiments, sutures were passed through the extraocular muscles to minimize convergent eye movements. The eye lids were held open with lid speculums and a contact lens was placed on the cornea. Obviously, these were not natural viewing conditions.

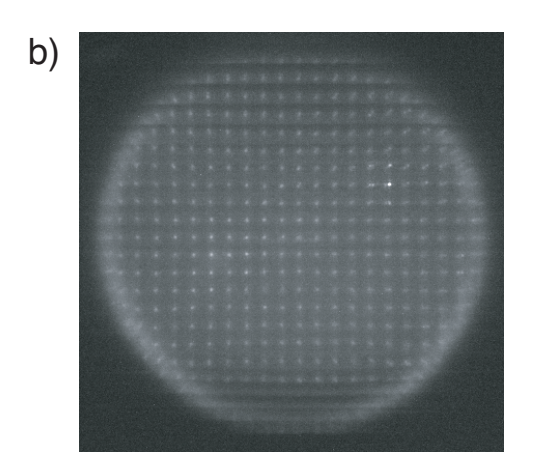
To understand the effects of these experimental interventions, aberrations were measured in each eye without sutures, speculum, or contact lens and again after the sutures and the lid speculum were inserted. This resulted in an increase in higher order aberrations (fifth to eighth Zernike orders). Aberrations were then measured again after the contact lens was placed on the cornea. The contact lens largely negated the increase in higher order aberrations caused by the sutures and speculum. The sign or amount of

baseline spherical aberration ($Z_{4,0}$) did not change after the contact lens was placed on the cornea.

Because the aberrations were measured through plano, rigid contact lenses on the corneas of both eyes, and because the contact lenses did not move with accommodation, all changes in ocular aberrations were due to changes in the lens only and not due to corneal changes (He, Gwiazda, Thorn, Held, & Huang, 2003; Yasuda, Yamaguchi, & Ohkoshi, 2003).

Changes in lenticular aberrations have been measured using a mechanical stretching apparatus (Glasser & Campbell, 1998) in isolated rhesus monkey and human lenses (Glasser, 2001; Roorda & Glasser, 1999; Roorda & Glasser, 2004). Although the mechanical stretching experiments do not mimic natural accommodation exactly, they do simulate the accommodative changes in the lens and can render the lens into accommodated and unaccommodated states. In the in vitro studies, negative spherical aberration of the isolated human and monkey lenses becomes more negative with accommodation (relaxation of stretching tension) (Glasser, 2001; Glasser & Campbell,





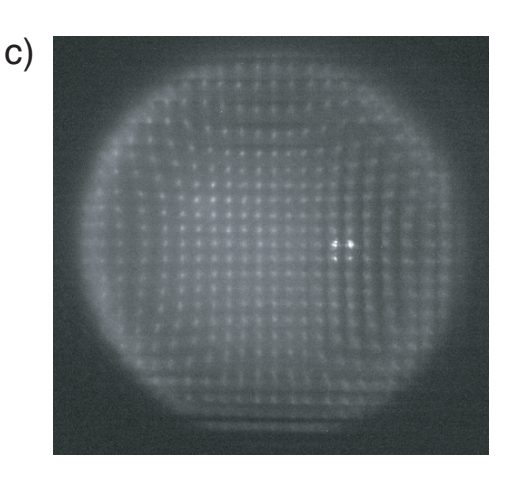


Figure 2. Video clip of dynamic changes in wavefront sensor image with accommodation (a). This video was recorded by a live capture of the Shack-Hartmann wavefront sensor (SHWS) image on the computer monitor during stimulation of accommodation in the experiment. A regular rectangular grid pattern of the SHWS image spots indicates low aberrations in the unaccommodated eye (b). However, when the eye accommodates, compression in the spot pattern, and hence change in optical power, is greatest at the center of the spot pattern with little or no change in the periphery (c).

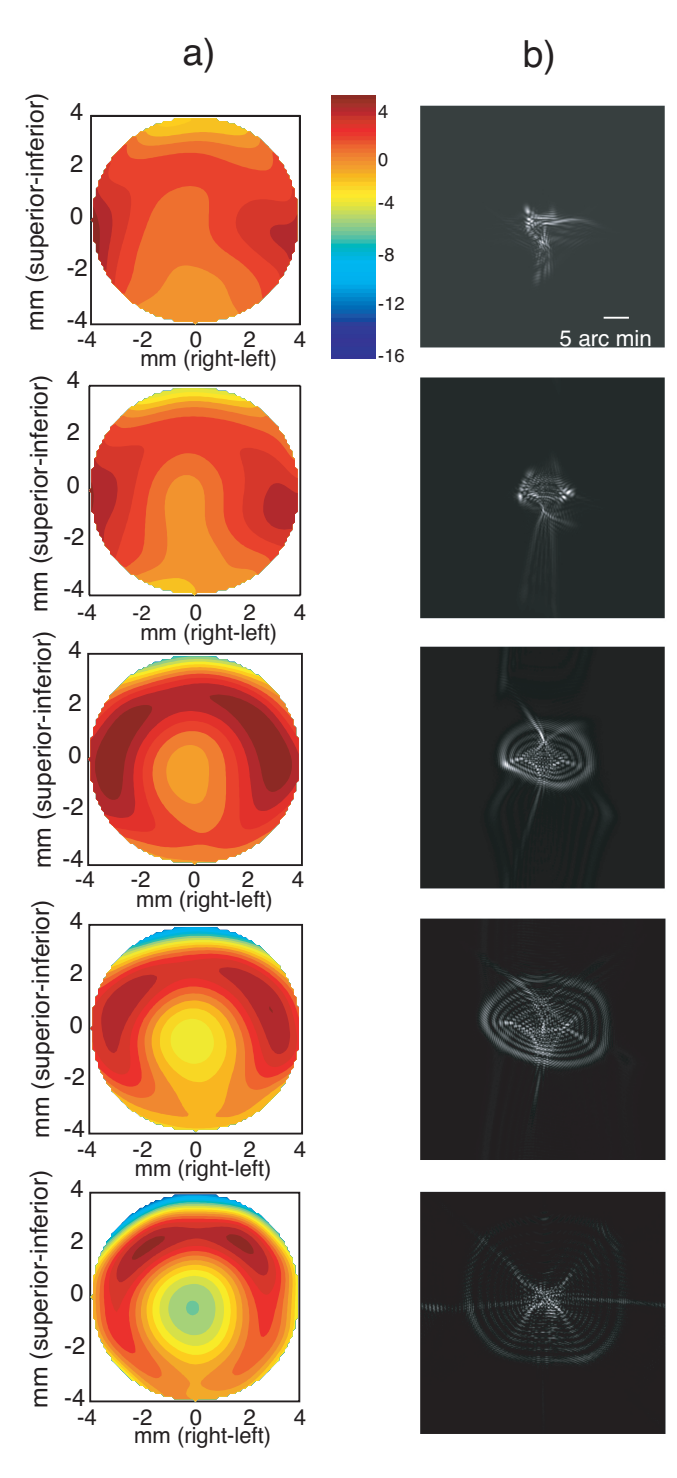


Figure 3. Wavefront maps (a) and PSFs (b), respectively, for the right eye for increasing accommodative amplitudes (0 D, 1.41 D, 3.88 D, 5.93 D, and 10.91 D). Wavefront maps (a) (with spherical defocus removed) show an accommodative increase in wave aberration with accommodation, particularly near the center of the eye for the highest amplitude. Each contour in the wavefront map indicates a 1-micron step, and a higher density of contours indicates a steeper wavefront in that region. PSFs (b) (defocus excluded) show a decrease in image quality over an 8-mm entrance pupil diameter. The false color scale is in units of microns and represents the color scale used for all wavefront maps.

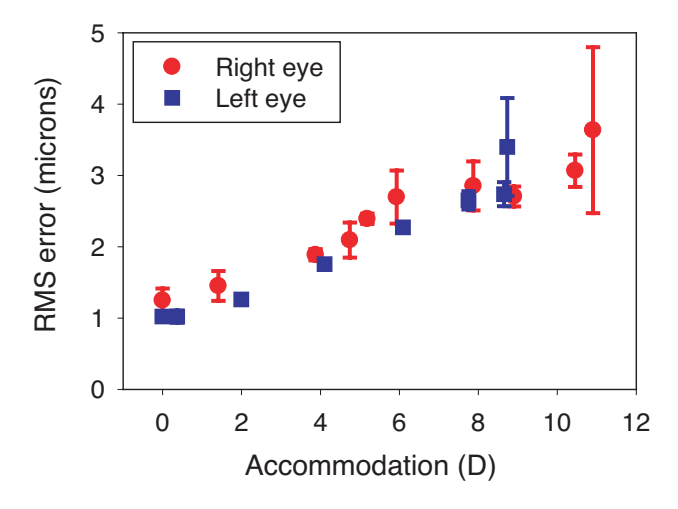


Figure 4. Change in RMS error of the wave aberration (excluding defocus) over an entrance pupil of 8 mm as a function of accommodative response calculated from the defocus ($Z_{2,0}$) term in the two eyes (circles, right eye; squares, left eye) of one rhesus monkey. Error bars represent SD of one measurement each from five images captured at each amplitude. Accommodative responses and amplitudes for the two eyes are not identical and were achieved using different stimulus currents for each eye.

1998; Roorda & Glasser, 1999; Roorda & Glasser, 2004). Here we show an increase in negative spherical aberrations with accommodation in vivo in rhesus monkey eyes. Although parallel rays are incident on the lens in vitro and convergent rays (after passing through the cornea) are incident on the lens in vivo, the end result, namely increase in spherical aberration in the negative direction, is similar. The similarity between the results from the in vivo and in vitro monkey lenses and between the in vitro human and in vitro monkey lenses suggests that the in vivo data obtained in the current study in monkey eyes are also likely to apply to human eyes.

A prior study in humans suggested that the best ocular image quality and consequently lowest aberrations occurred around the resting state of ocular accommodation (He et al., 2000). In this study, however, higher order ocular aberrations increased systematically with accommodation at all accommodative states in the two eyes. The monkey eyes showed slight negative spherical aberration in the unaccommodated state, which became progressively more negative with accommodation. Although aberrations in the monkey eyes were measured through the contact lenses, the sign or amount of baseline symmetrical spherical aberration did not change systematically before and after placing the contact lenses on the corneas. Some human subjects in the He et al. study had positive spherical aberration in the unaccommodated state, and with accommodation, the spherical aberration would go from positive through zero to negative spherical aberration, which would minimize the total wavefront error at a mildly accommodated state.

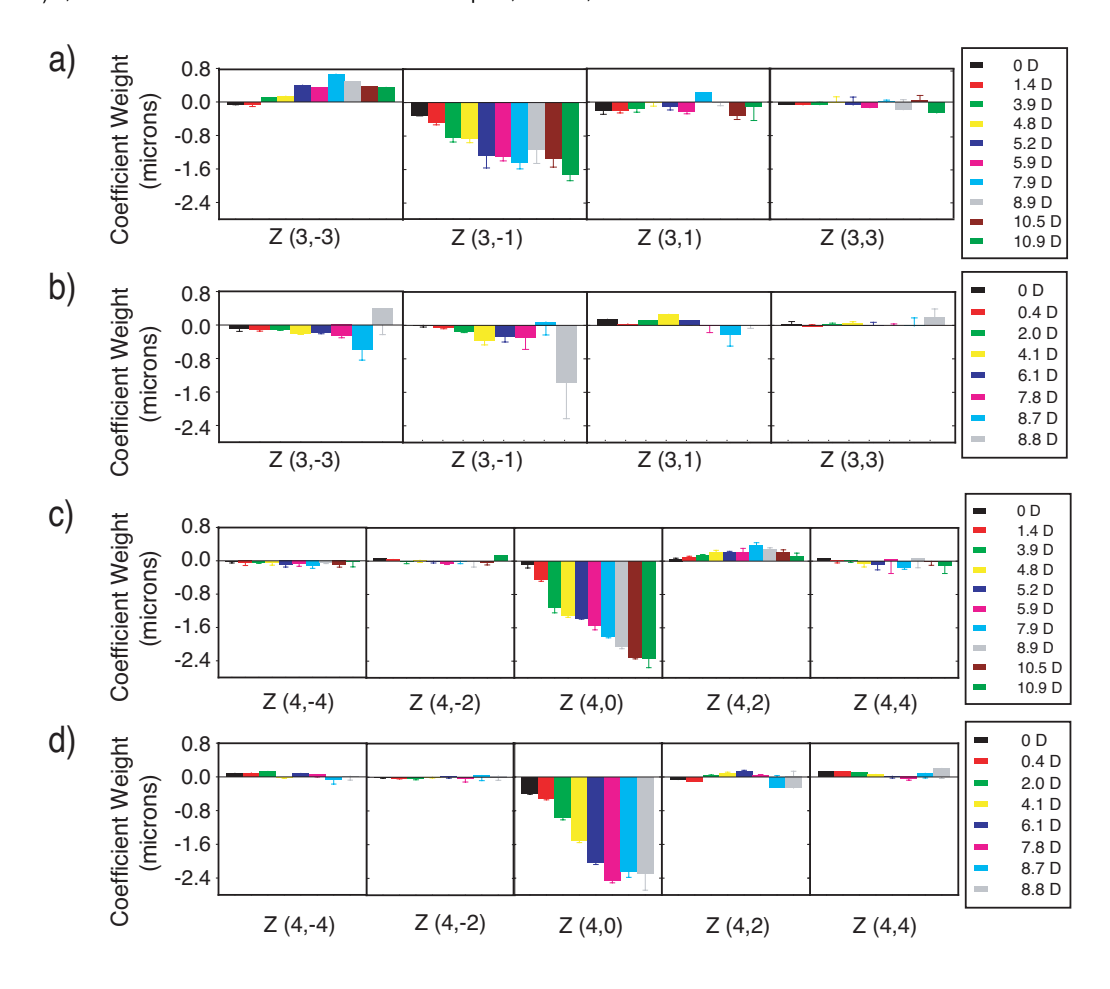


Figure 5. Accommodative change in vertical coma (a & b) and forth-order spherical aberration (c & d) terms in the right (a & c) and the left (b & d) eyes as a function of accommodative response calculated from the defocus ($Z_{2,0}$) term. There is a significant increase in vertical coma at the highest amplitudes in the two eyes. Spherical aberration becomes systematically more negative with increasing amplitude of accommodation.

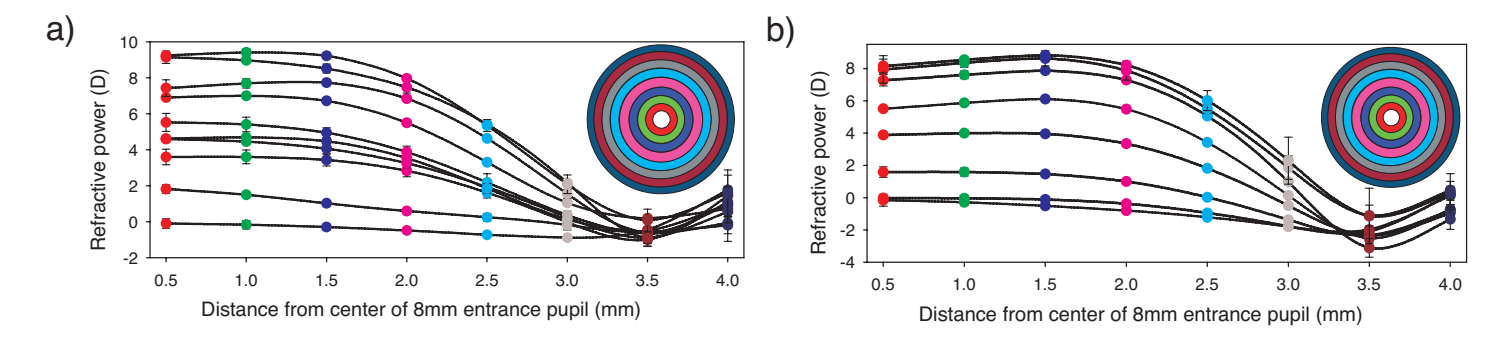


Figure 6. Refractive power calculated from curvature maps from center to periphery over 8-mm entrance pupil diameters in the right (a) and the left (b) eyes. Red, green, blue, pink, cyan, gray, dark red, and dark blue symbols represent mean calculated power at concentric annuli of eccentricities of 0.5, 1, 1.5, 2, 2.5, 3, 3.5, and 4 mm, respectively, from the center of the curvature map at the different accommodative states. The inset diagrams depict the color-coded annuli of the pupil sampled to compute accommodative power from the curvature map at each concentric sub-region. Error bars indicate SDs from five measures obtained from five images. Lines connecting the symbols depict data obtained from the analysis of a single image from a particular stimulus current amplitude. Refractive power at each concentric annular region was calculated for the unaccommodated (0 μ A) state and at each increasing accommodative state in both eyes.

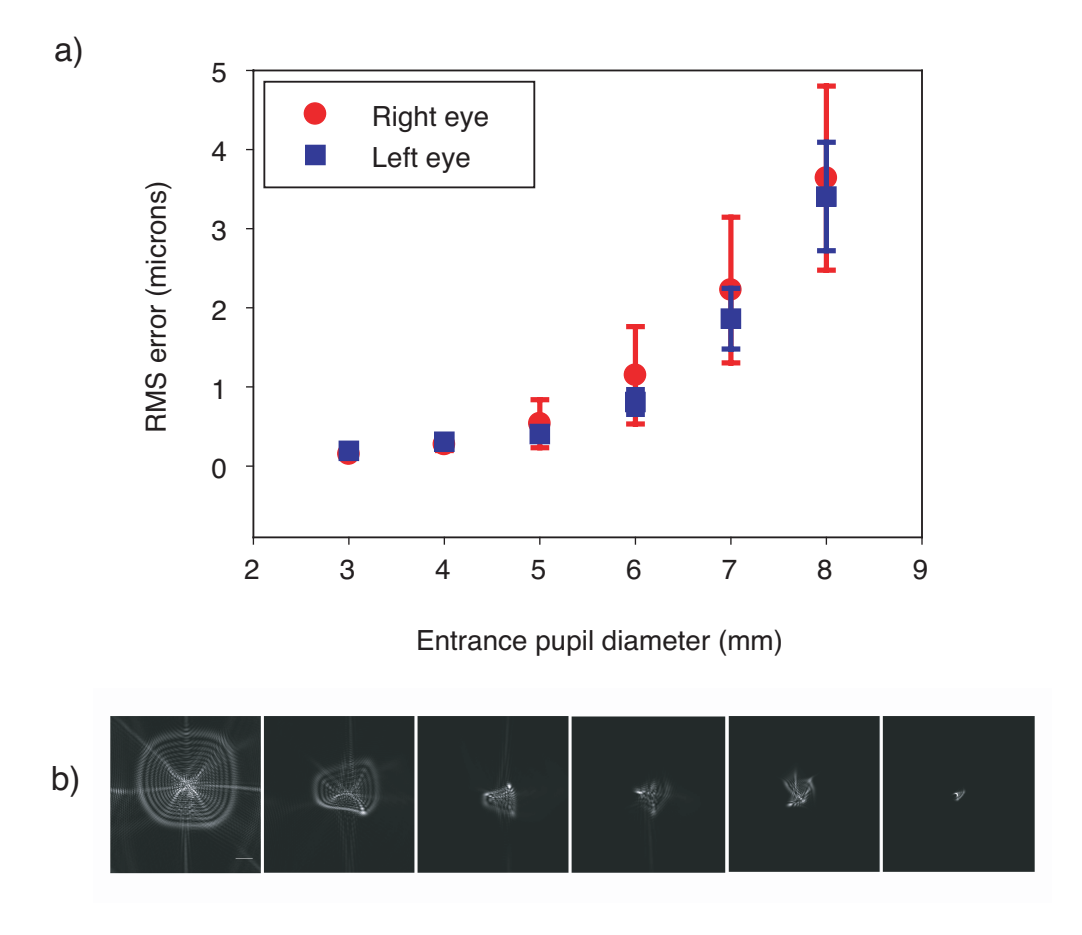


Figure 7. (a). Change in RMS error of the wave aberration at the highest accommodated state of approximately 11 D in the right eye (circles) and 9 D in the left eye (squares) with increasing entrance pupil diameter from 3 mm to 8 mm. Error bars represent *SD* from measurements on five separate SHWS images captured at the maximum accommodated state for each eye. PSFs at maximum accommodation in the right eye calculated for entrance pupil diameters of 8, 7, 6, 5, 4, and 3 mm. (b). The decrease in width of the PSF indicates an improvement in image quality with a reduction in entrance pupil diameter. Scale bar = 5 arcmin.

Here, symmetric spherical aberration $(Z_{4,0})$ changed systematically and significantly with accommodation, and vertical coma $(Z_{3,-1})$ while changing significantly in the two monkey eyes, changed systematically in the right eye only. In the previous study in humans, some subjects showed a systematic increase in vertical coma, whereas others did not (He et al., 2000). The increase in vertical coma over the 8mm entrance pupil diameter with accommodation could be due to a decentered change in power of the lens, a lateral movement of the lens with respect to the cornea, a tilt or sag of the lens, or a combination of all four factors. Accommodative changes in ocular aberrations, although likely to be most strongly influenced by changes in lens shape, could also be influenced by a combination of changes in lens shape, posterior corneal to anterior lens distance, and lens gradient refractive index distribution (Garner & Smith, 1997; Gullstrand, 1924). Total ocular wave aberration measurements cannot be used to distinguish between the relative contributions of these factors.

The curvature analysis over the entire lens diameter at increasing amplitudes (Figure 6a & 6b) demonstrates the

spatially variant changes in lens power during accommodation. Optical power change is pronounced and relatively uniform over the central 3 mm but decreases rapidly beyond that out to the lens periphery. The inflection point beyond 7-mm diameter in both eyes at all amplitudes is interesting. This is likely due to the fact that the aberrations are being measured out very near to the equatorial edge of the lens. Because the curvature of the lens increases progressively toward the equator, there is an expected progressive increase in power. This is evident by the fact that the sixth-order spherical aberration term ($Z_{6,0}$) is significant and positive at all amplitudes and does not change with accommodation. The center/periphery dichotomy in change in optical power with accommodation is evident as an increase in negative spherical aberration during accommodation (Figure 5c & 5d). To simulate normal accommodative pupillary miosis in the iridectomized eyes, SHWS spot patterns were analyzed at the highest amplitudes of accommodation in the two eyes over decreasing entrance pupil diameters ranging from 8 to 3 mm in 1-mm steps. This analysis showed that aberrations decreased and consequently

image quality improved with decreasing entrance pupil diameter. The increase in aberrations with accommodation (Figure 3) due to the spatially variant changes in the lens would be offset by a decrease in aberrations due to an accommodative pupil constriction that would occur with the iris present in a normal eye (Figure 7). Accommodative pupil constriction would thereby serve to maximize the overall ocular accommodative refractive change by allowing passage of the relatively more powerful paraxial rays while blocking the relatively less powerful peripheral rays (Figure 6a & 6b) and would also serve to maintain good image quality.

Conclusions

These results show that with an accommodative decrease in equatorial diameter of the lens, there is a greater power change at the central region of the eye than in the periphery. This is consistent with the lens undergoing a greater increase in curvature at the center, but a reduced change in curvature, or even flattening, in the periphery. A similar result is seen in the in vitro optical measurements on isolated rhesus monkey lenses when mechanical stretching tension is released (Roorda & Glasser, 2004). These results provide harmony to the apparent discord between the accommodative mechanisms of Tscherning (Schachar et al., 1995; Tscherning, 1920), on the one hand, and Helmholtz (Helmholtz, 1924), Gullstrand (Gullstrand, 1924), and Fincham (Fincham, 1937b) on the other.

Direct observations of the accommodative decrease in lens diameter (Figure 1) in conjunction with knowledge of how the optical aberrations change over the full lens diameter (Figures 2, 4, and 6) provide compelling evidence that the lens does not simply become more spherical with accommodation. A hypothesis that can explain the spatially variant changes seen in this experiment is that one or both of the lens surfaces undergo aspheric changes in curvature during accommodation. However, the changes in aberrations observed may also in part be due to variations in the lenticular gradient refractive index during accommodation. The study performed here does not distinguish between these possible contributing factors. Such a mechanism whereby accommodative lens power is maximized at the center, possibly as a consequence of regional variation in capsular thickness, allows the monkey lens to undergo significant increases in accommodative power at the center with only a relatively small decrease in diameter. The regional variations in capsular thickness described by Fincham (1937b) in the primate lens provide an intuitively satisfying explanation for how the capsule may mould the lens to undergo these accommodative shape changes to produce the optical effect reported here. This accommodative change in the form of the crystalline lens is profoundly different from the simple spherical accommodative change that the primate lens has traditionally been assumed to undergo.

Acknowledgments

Thanks to Chris Kuether and Hope Queener for technical assistance and Ming Le and Siddharth Poonja for computer programming. This work was funded in part from a grant from Pharmacia, Groningen, and NIH Grant #1 RO1 EY 014651-01 to AG and in part by a grant from Pharmacia, Groningen, to AR.

Commercial Relationships: none.

Corresponding author: Adrian Glasser.

Email: aglasser@uh.edu.

Address: College of Optometry, University of Houston,

Houston, TX, USA.

References

- Atchison, D. A., Collins, M. J., Wildsoet, C. F., Christensen, J., & Waterworth, M. D. (1995). Measurement of monochromatic ocular aberrations of human eyes as a function of accommodation by the Howland aberroscope technique. *Vision Research*, *35*, 313-323. [PubMed]
- Bito, L. Z., Kaufman, P. L., DeRousseau, C. J., & Koretz, J. (1987). Presbyopia: An animal model and experimental approaches for the study of the mechanism of accommodation and ocular aging. *Eye*, 1, 222-230. [PubMed]
- Crawford, K., Terasawa, E., & Kaufman, P. L. (1989). Reproducible stimulation of ciliary muscle contraction in the cynomolgus monkey via a permanent indwelling midbrain electrode. *Brain Research*, 503, 265-272. [PubMed]
- Crawford, K. S., Kaufman, P. L., & Bito, L. Z. (1990). The role of the iris in accommodation of rhesus monkeys. *Investigative Ophthalmology and Visual Science*, 31, 2185-2190. [PubMed]
- Croft, M. A., Kaufman, P. L., Crawford, K. S., Neider, M. W., Glasser, A., & Bito, L. Z. (1998). Accommodation dynamics in aging rhesus monkeys. *The American Journal of Physiology*, 275, R1885-R1897. [PubMed] [Article]
- Cubalchini, R. (1979). Modal wave-front estimation from derivative measurements. *Journal of the Optical Society of America*, 69, 972-977.
- Fincham, E. F. (1937a). The coincidence optometer. *Procedures of the Physiological Society of London*, 49, 456-468.
- Fincham, E. F. (1937b). The mechanism of accommodation. *The British Journal of Ophthalmology*, Monograph VIII, 7-80.
- Garner, L. F., & Smith, G. (1997). Changes in equivalent and gradient refractive index of the crystalline lens with accommodation. Optometry and Vision Science, 74, 114-119. [PubMed]

- Glasser, A. (2001). Accommodative optical changes in the primate crystalline lens [Abstract]. *Investigative Ophthalmology and Visual Science*, 53, B26.
- Glasser, A., & Campbell, M. C. W. (1998). Presbyopia and the optical changes in the human crystalline lens with age. *Vision Research*, 38, 209-229. [PubMed]
- Glasser, A., & Kaufman, P. L. (1999). The mechanism of accommodation in primates. *Ophthalmology*, 106, 863-872. [PubMed]
- Gullstrand, A. (1924). Mechanism of accommodation. In J. P. C. Southall (Ed.), *Helmholtz's treatise on physiological optics* (382-415). The Optical Society of America. (Translated from the 3rd German edition, 1909)
- He, J. C., Burns, S. A., & Marcos, S. (2000). Monochromatic aberrations in the accommodated human eye. *Vision Research*, 40, 41-48. [PubMed]
- He, J., Gwiazda, J., Thorn, F., Held, R., & Huang, W. (2003). Change in corneal shape and corneal wavefront aberrations with accommodation. *Journal of Vision*, 3(7), 456-463, http://journalofvision.org/3/7/1/, doi:10.1167/3.7.1. [PubMed] [Article]
- Helmholtz von, H. H. (1924). Mechanism of accommodation. In J. P. C. Southall (Ed.), Helmholtz's treatise on physiological optics (143-173). The Optical Society of America. (Translated from the 3rd German edition, 1909)
- Ivanoff, A. (1947). On the influence of accommodation on spherical aberration in the human eye, an attempt to interpret night myopia. *Journal of the Optical Society of America*, 37, 730-731.
- Jenkins, T. C. A. (1963). Aberrations of the eye and their effects on vision. Part 1. *The British Journal of Physiological Optics*, 20, 59-91. [PubMed]
- Kaufman, P. L., & Lütjen-Drecoll, E. (1975). Total iridectomy in the primate in vivo: Surgical technique and postoperative anatomy. *Investigative Ophthalmology and Visual Science*, 14, 766-771. [PubMed]
- Koomen, M., Tousey, R., & Scolnik, R. (1949). The spherical aberration of the eye. *Journal of the Optical Society of America*, 39, 370-376.
- Liang, J., Grimm, B., Goelz, S., & Bille, J. F. (1994). Objective measurement of wave aberrations of the human eye with the use of a Hartmann-Shack wave-front sensor. *Journal of the Optical Society of America A*, 11, 1949-1957. [PubMed]
- Liang, J., & Williams, D. R. (1997). Aberrations and retinal image quality of the normal human eye. *Journal of the Optical Society of America A*, 14, 2873-2883. [PubMed]
- Lopez-Gil, N., Iglesias, I., & Artal, P. (1998). Retinal image quality in the human eye as a function of the accommodation. *Vision Research*, 38, 2897-2907. [PubMed]

- Ninomiya, S., Fujikado, T., Kuroda, T., Maeda, N., Tano, Y., Oshika, T., Hirohara, Y., & Mihashi, T. (2002). Changes of ocular aberration with accommodation. *American Journal of Ophthalmology*, 134, 924-926. [PubMed]
- Pallikaris, L. G., Panagopoulou, S. I., Siganos, C. S., & Molebny, V. V. (2001). Objective measurement of wavefront aberrations with and without accommodation. *Journal of Refractive Surgery*, 17, S602-S607. [PubMed]
- Roorda, A., & Glasser, A. (1999). In vitro wavefront aberration measurements of isolated crystalline lenses [Abstract]. Presented at the Optical Society of America Annual Meeting, Washington, D.C.
- Roorda, A., & Glasser, A. (2004). Wave aberrations of the isolated crystalline lens. *Journal of Vision*, *4*(4), 250-261, http://journalofvision.org/4/4/1/, doi:10.1167/4.4.1. [PubMed] [Article]
- Schachar, R. A., Black, T. D., Kash, R. L., Cudmore, D. P., & Schanzlin, D. J. (1995). The mechanism of accommodation and presbyopia in the primate. *Annals of Ophthalmology*, 27, 58-67.
- Schachar, R. A., Tello, C., Cudmore, D. P., Liebmann, J. M., Black, T. D., & Ritch, R. (1996). In vivo increase of the human lens equatorial diameter during accommodation. *The American Journal of Physiology*, 271, R670-R676. [PubMed]
- Strenk, S. A., & Semmlow, J. L. (1995). Magnetic resonance images of the ciliary muscle and lens in presbyopes and non-presbyopes. *Vision Science and Its Applications* (pp. 88-91). Washington, D.C.: Optical Society of America.
- Thibos, L. N., & Applegate, R. A. (2001). Assessment of optical quality. In S. M. MacRae, R. R. Krueger, & R. A. Applegate (Eds.), Customized corneal ablation: The quest for supervision (pp. 67-78). New Jersey: SLACK, Inc.
- Thibos, L. N., Applegate, R. A., Schwiegerling, J. T., Webb, R., & VSIA Standards Taskforce Members (2001). Standards for reporting the optical aberrations of eyes. In S. M. MacRae, R. R. Krueger, & R. A. Applegate (Eds.), Customized corneal ablation: The quest for supervision (pp. 348-361). New Jersey: SLACK, Inc.
- Tscherning, M. (1920). Accommodation. *Physiologic Optics* (pp. 192-228). Philadelphia: The Keystone.
- van den Brink, G. (1962). Measurements of the geometrical aberrations of the eye. Vision Research, 2, 233-244.
- Vilupuru, A. S., & Glasser, A. (2002). Dynamic accommodation in rhesus monkeys. *Vision Research*, 42, 125-141. [PubMed]

- Wilson, R. S. (1997). Does the lens diameter increase or decrease during accommodation? Human accommodation studies: A new technique using infrared retroillumination video photography and pixel unit measurements. *Transactions of the American Ophthalmological Society*, 95, 261-267. [PubMed]
- Yasuda, A., Yamaguchi, T., & Ohkoshi, K. (2003). Changes in corneal curvature in accommodation. *Journal of Cataract and Refractive Surgery*, 29, 1297-1301. [PubMed]
- Young, T. (1801). On the mechanism of the eye. *Philosophical Transactions of the Royal Society of London*, 91, 23-88.